Mem. S.A.It. Vol. 81, 806

Memorie della

Coupling photosphere and chromosphere through plasma waves

M. Stangalini[1], F. Berrilli[1], D. Del Moro[1], A. Egidi[1], S. Giordano[2], P. F. Moretti[3], and B. Viticchiè[1]

[1] Università degli studi di Roma "Tor Vergata", Via della Ricerca Scientifica 1, I-00133 Rome, Italy, e-mail: marco.stangalini@roma2.infn.it
[2] Altran Italia SpA
[3] CNR P.le A. Moro 7 - I-00185 Rome, Italy

Abstract. The new capabilities of fast bidimensional spectropolarimetric scanning, allowed by recent instrumental development, provide a new insight into the study of chromospheric active regions. We present results from the analysis of datasets acquired with Interferometric BIdimensional Spectrometer operating at the Dunn Solar Telescope in spectrometric and spectropolarimetric mode. The high spatial and temporal resolution allows us to study oscillations and MHD wave propagation between photosphere and chromosphere. In particular we focused on the coupling between photospheric magnetic field and wave transmission. Among other findings, we observe a shift of the cross-correlation spectrum, above those photospheric regions where the magnetic field vector is strongly inclined with respect to the line of sight. Such a result could offer a new perspective for the understanding of plasma wave reprocessing.

Key words. Sun: magnetic fields – Sun: oscillations

1. Introduction

Magnetic field inclination has been identified as one of the causes of cutoff frequency shift for acoustic waves (Jefferies et al. 2006; McIntosh & Jefferies 2006; Cally & Schunker 2006). More specifically, it has been shown that the cutoff frequency $\nu_{\mathrm{cutoff}} = \gamma g/4\pi c = 5.2$ mHz can be lowered below this value due to magnetic field inclination (Bel & Leroy 1977) in regions where the plasma parameter $\beta << 1$.

This can allow the transmission of waves with frequencies below 5.2 mHz.

Send offprint requests to: M. Stangalini

Acoustic waves are also found to interact with the canopy around magnetic structures (Moretti et al. 2007).

An alternative scenario for such a lowering in the cutoff frequency for acoustic waves can be found in radiative losses that can occur in the photosphere (Roberts 1983).

In this work we present a study of the properties of acoustic waves propagation and we compare these to magnetic field geometry inferred from full Stokes signals of a magnetic structure acquired with the Interferometric Bidimensional Spectrometer (IBIS) installed at the Dunn Solar Telescope in the Fe 617.3 nm and Ca 854.2 nm lines. We find that 3 mHz

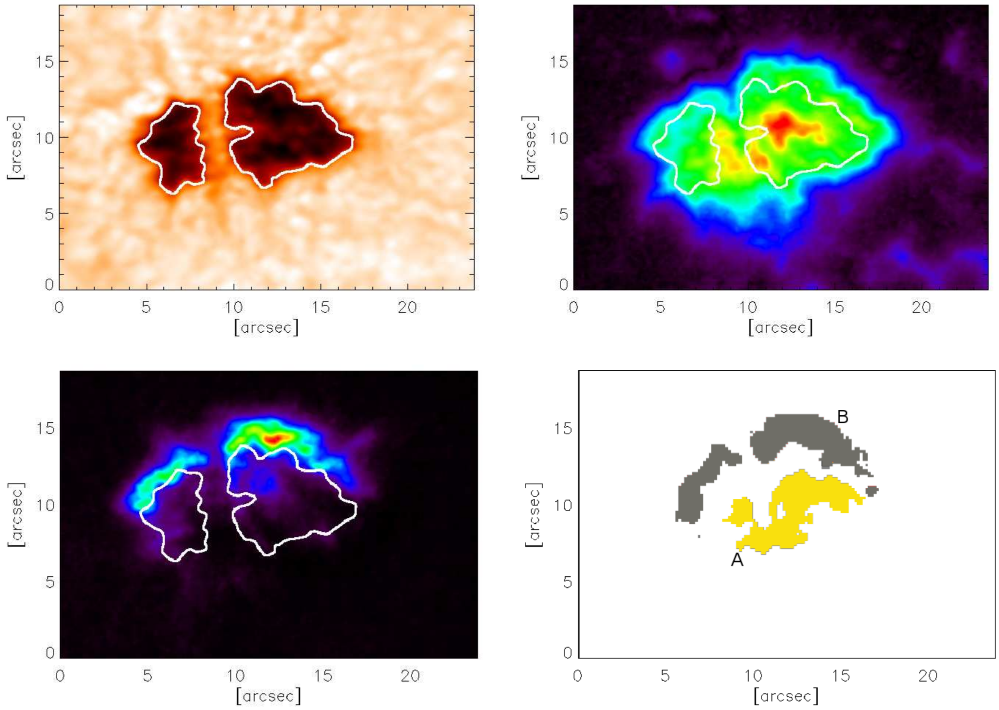

Fig. 1. Upper left panel: the average continuum image at ~ 617.3 nm with an isophote defining the sunspot contour overplotted. Upper right panel: the integrated circular polarized component of the incoming radiation associated to the Fe I 617.3 nm line. Lower left panel: the integrated linear polarized component of the incoming radiation associated to the Fe I 617.3 nm line. Lower right panel: Selected regions for the analysis of wave transmission. Region A indicates the region where the Stokes V is greater than 3σ threshold and B is the region where the $U + Q$ signal is greater than a 3σ threshold. On all images the same isophote of the average continuum image is overplotted.

waves propagate upward mainly in the region surrounding the magnetic structure forming a ring shaped region outside the umbra, while 5 mHz waves propagate at the borders of the umbra. We also find that the cross-correlation spectrum is fairly affected by the field geometry, showing a shift toward low frequencies (3 mHz) in those regions where the magnetic field is strongly inclined with respect to the Line-of-Sight (LoS) and the U and Q Stokes signals concentrate.

2. Observations and data analysis

The observation run was performed 2008 October 15 in full-Stokes mode with IBIS. IBIS is based on a dual Fabry-Pérot interferometric system. It combines high spectral resolution with short exposure times and a large field of view, as well as the ability to measure the polarization (Cavallini 2006).

The region tracked was the AR11005 which, seen in SOHO and Hinode images, appears as a small bipolar region in the northern hemisphere at high latitude (≃ 30° N), belonging to the new magnetic cycle. We observed the only structure evident in continuum light, at [25.2° N, 10.0° W]. Such a structure is a sunspot, probably in the decay phase, which exhibits a light-bridge and several umbral-dots (upper left panel in Fig. 1). Spectopolarimetric observations (upper right and lower left panels in Fig. 1) reveal that the magnetic field leans towards the photosphere in the upper part of the structure (towards disk center), however a penumbral structure is not visible in broad-band images.

The dataset consists of 80 sequences, containing a full Stokes 21 points scan of the Fe 617.3 nm line and a 21 points scan of the Ca 854.2 nm line. The wavelength distance in between the spectral points for the Fe line is 20.0 mÅ. The wavelength distance in between the spectral points for the Ca line is 60.0 mÅ. The exposure time for each image was set to 80 ms and each spectral scan took 52 seconds to complete, thus setting the time resolution. The pixel scale of these 512 × 512 pixel images was set at $0\farcs167$. For each spectral image a broad-band (WL) and a G-Band counterpart, approximately imaging the same FOV, have been acquired as ancillary images. The pixel scale of the 1024 × 1024 pixel WL image (621.3 ± 5 nm) was set at $0\farcs0835$ and the exposure time was 80 ms (shared shutter with IBIS spectral images).The pixel scale of the 1024 × 1024 pixel G-band image (430.5 ± 0.5 nm) was set at $0\farcs0514$ and the integration time was 10 ms.

The pipeline provided by the IBIS team takes care of normal calibration processes (dark frame, flat field, etc.) and also corrects for blue-shift effects (Reardon & Cavallini 2008) and instrumental polarization. For further details on the calibration pipeline see Viticchiè et al. (2009).

The ancillary images have been restored with Multi-Frame Blind Deconvolution (MFBD) (van Noort et al. 2005), obtaining a single frame for each scan both for the G-band and the broad-band images. Using these images, the spectropolarimetric images have been registered and destretched to fix the AO uncorrected seeing effects and to achieve the highest spatial resolution.

The estimated mean spatial resolution of the LoS velocity fields computed from the spectropolarimetric scans used in this work is $0\farcs36$.

3. Cross-correlation spectra

Using the LoS velocity fields for both the Fe 617.3 nm and Ca 854.2 nm lines, we studied the cross-correlation spectrum and the phase lag, focusing on two regions: one with strong circular polarization and one with strong linear polarizations signals.

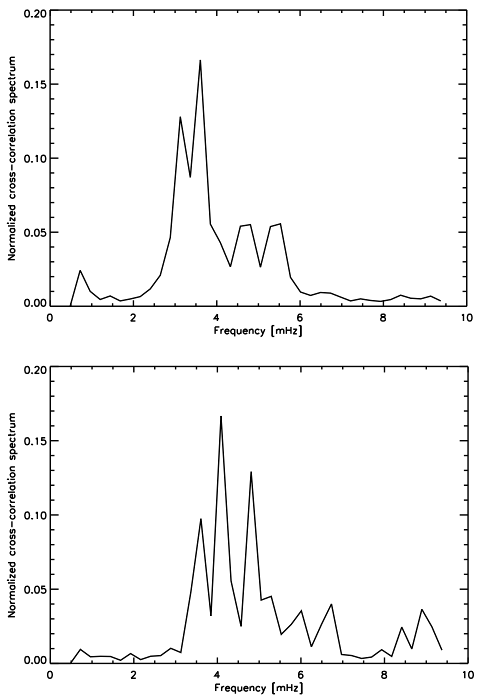

Fig. 2. Cross-correlation spectrum obtained in the region where the magnetic field is highly linearly polarized (upper panel) and highly circularly polarized (lower panel). Low-frequency peaks at 0.5 and 1 mHz have been filtered out as they are caused by seeing conditions modulations as deduced by further analysis (not reported here). The sampling time scale is 52 s and dataset duration is 70 minutes.

Despite the complexity of line formation in a highly structured atmosphere, Doppler shifts of the line Ca 854.2 nm are a reliable diagnostic of the low-chromosphere (Vecchio et al. 2007) We selected two regions (see Fig. 1) setting a 3σ threshold on $U + Q$ Stokes signals (region B in the lower right panel of Fig. 1) and on V Stokes (region A in the lower right panel of Fig. 1).

This selection allows us to study the waves propagation in two different regimes of magnetic field inclination.

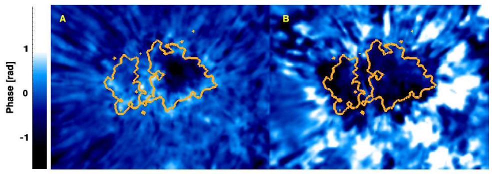

Fig. 3. Phase map for 5 mHz component (panel A) and for 3 mHz (panel B).

It is worth noting how the linear polarization signal is not symmetric with respect to the magnetic structure center and it is mainly outside the visible umbra edges.

From this analysis we obtained the cross-correlation spectra shown in Fig. 2.

As evident, the spectrum shape is dependent on the region analyzed. Pixels with inclined magnetic field (region B in Fig. 1) show a higher cross-correlation amplitude at lower frequency (~ 3.5 mHz) with respect to the region where the polarization is mainly circular (region A in Fig. 1). This umbral region shows the highest peaks in the cross-correlation spectrum at higher frequencies, between 4 mHz and 5.5 mHz.

4. Phase lag

We investigated the phase lag between the photosphere and chromosphere at small spatial scales in and around the magnetic structure. In Fig. 3 the phase maps corresponding to 5 mHz (panel A) and 3 mHz (panel B) components are reported.

The maps clearly show that the 3 mHz waves are propagating upward (phase greater than zero) mainly around the magnetic structure. Whereas, 5 mHz waves are propagating upward at the edges of the umbra and in the left lobe of the sunspot.

This scenario seems to be compatible with that described by de Wijn et al. (2009). The authors reported that 3 mHz waves propagated mostly in regions surrounding magnetic structures where the field is most likely to be inclined, thus contributing to the cutoff frequency shift.

Acknowledgements. We thank Alexandra Tritschler for providing the IBIS data reduction pipeline. IBIS was built with contributions from INAF/Arcetri Observatory, the University of Florence, the University of Rome Tor Vergata, and MIUR. NSO is operated by the Association of Universities for Research in Astronomy, Inc. (AURA), under cooperative agreement with the National Science Foundation.

References

Bel, N. & Leroy, B. 1977, A&A, 55, 239

Cally, P. S. & Schunker, H. 2006, in Beyond the spherical Sun, ed. K. Fletcher & M. Thompson, Proceedings of SOHO 18/GONG 2006/HELAS I, ESA Special Publication, 624, Published on CDROM

Cavallini, F. 2006, Sol. Phys., 236, 415

de Wijn, A. G., McIntosh, S. W., & De Pontieu, B. 2009, ApJ, 702, L168

Jefferies, S. M., McIntosh, S. W., Armstrong, J. D., et al. 2006, ApJ, 648, L151

McIntosh, S. W. & Jefferies, S. M. 2006, ApJ, 647, L77

Moretti, P. F., Jefferies, S. M., Armstrong, J. D., & McIntosh, S. W. 2007, A&A, 471, 961

Reardon, K. P. & Cavallini, F. 2008, A&A, 481, 897

Roberts, B. 1983, Sol. Phys., 87, 77

van Noort, M., Rouppe van der Voort, L., & Löfdahl, M. G. 2005, Sol. Phys., 228, 191

Vecchio, A., Cauzzi, G., Reardon, K. P., Janssen, K., & Rimmele, T. 2007, A&A, 461, L1

Viticchiè, B., Del Moro, D., Berrilli, F., Bellot Rubio, L., & Tritschler, A. 2009, ApJ, 700, L145